

BaTiO<sub>3</sub>의 광학적 특성과 동적 홀로그램의 응용

김기현, 김기현, 김기현

한국통신학회, 서울, 1988년 11월 5일

본 논문은 한국통신학회에서 지원한 연구의 결과이다. 본 논문은 한국통신학회에서 지원한 연구의 결과이다.

ABSTRACT

A brief review of properties of photorefractive material for optical data processing is given. Based on frequency-plane correlator scheme, a real-time pattern recognition system using dynamic hologram in photorefractive BaTiO<sub>3</sub> is presented, and some methods for enhancing pattern discrimination are proposed. Examples of optical pattern recognition for military patterns are performed and discussed.

1. INTRODUCTION

Demands for large bandwidth and rapid processing of information have caused attention to optical signal processing since the early work performed by Vander Lugt<sup>(1)</sup>. Many experimental systems have been demonstrated which rely on the use of wet-processed holographic matched filters, but conventional pattern recognition techniques are somewhat ineffective in that filters can not be changed at a speed comparable with the processing time of the correlator because of time-consuming development step and critical setup. The use of the photorefractive medium-based dynamic hologram such as BaTiO<sub>3</sub> and BSO in place of the classical holographic filter is one possible solution to these problems.

Since the photorefractive effect was first noticed in LiNbO<sub>3</sub><sup>(2)</sup>, holographic storage<sup>(3)</sup>, edge enhancement<sup>(4)</sup> and correlation-convolutions<sup>(5)</sup> have been demonstrated. And optical logic processor and coherent image amplifier have been proposed.

Optical pattern recognition system can be divided into two regimes: logic-based digital pattern recognition and correlative pattern recognition system. Logic based pattern recognition offers higher accuracy and flexibility, but speed and bandwidth requirement restrict its applications.

In this paper, several aspects of real-time volume hologram employing BaTiO<sub>3</sub> single crystal as a photorefractive material are briefly reviewed, and methods of discrimination enhancement are presented. Then the implementation of pattern recognition system and experimental results are presented.

2. DYNAMIC CORRELATOR

2.1. Material Properties for ODP

The most general and the useful formulation of the photorefractive effects emerged from Kukhtarev in 1979.<sup>(6)</sup> This band transport model is summarized as four interdependent equations: continuity, rate equation, current equation and Poisson's law. By using these equations, some figures of merit for photorefractive material such as steady-state index change, the response time and diffraction efficiency can be derived.

In the steady-state and for small modulation ( $m \ll 1$ ), the index change is related directly to the space charge field through

$$\Delta n = 1/2 \times n_b^3 r_{eff} m E_{sc} \tag{1}$$

where

$$E_{sc} = E_q \left| \frac{E_0^2 + E_D^2}{E_0 + (E_D^2 + E_q^2)} \right| \tag{2}$$

(E<sub>0</sub> = applied field)

and background index of BaTiO<sub>3</sub> crystal is 2.4 when E<sub>0</sub> = 0 and E<sub>D</sub> < E<sub>q</sub>,

$$E_{sc} \cong E_D = \frac{k_B T k_g}{e} \tag{3}$$

In case of  $\lambda_g > 1.5$  to  $5 \mu m$ , steady-state index change is order of  $10^{-3}$  which is 20 to 50 times larger than that in BSO.

Response time of the crystal is given by

$$t_{min} = (\hbar W / I_0 \alpha \eta) N \propto 1/I_0 \quad (4)$$

In BaTiO<sub>3</sub> crystal, response time with no applied field is faster than with applied field and order of 100 ns which is 100 times longer than BSO crystal.

Another important figure of merit, i.e., diffraction efficiency of the holographic grating is given by

$$\eta \approx \left| \frac{\pi \Delta n l}{\lambda} \right|^2 \quad (5)$$

Diffraction efficiency of BaTiO<sub>3</sub> is somewhat lower than BSO crystal but can be enhanced by adopting larger crystal length l.

From above discussions, it is easily seen that BSO is a fast and sensitive with a relatively small electro-optic coefficient. On the other hand, BaTiO<sub>3</sub> has large electro-optic coefficients and is highly efficient, but responds rather slowly.

## 2.2. Principle of Dynamic Correlator

So far we have discussed the basic properties of photorefractive materials. We will now consider how photorefractive material can be used as a dynamic correlator. Fig.1 shows the four wave mixing geometry employing photorefractive material as the recording media. In the Figure, fields E<sub>1</sub> and E<sub>2</sub> are the pump beams, E<sub>4</sub> is the probe beam and E<sub>3</sub> is the output, which are given by

$$E_1 = A_1(r) \exp(i\omega t - k_1 r) \\ k_1 + k_2 = 0 \quad (6)$$

Mixing these three inputs in a photorefractive medium produces an output field, and it can be derived by coupled-wave equations:

$$\frac{d A_3}{d z} \approx \frac{\gamma}{I_0} A_1 A_2 A_4^* \quad (7)$$

where the asterisk denotes the complex conjugate,  $\gamma$  is the photorefractive coupling constant, I<sub>0</sub> is the total intensity. If we render beam E<sub>2</sub> incoherent with respect to E<sub>1</sub> and E<sub>4</sub> by proper adjusting the optical path length of beam E<sub>2</sub>, the output or scattered amplitude A<sub>3</sub> will be proportional to

$$A_3 \propto A_1 A_2 A_4^* \quad (8)$$

Above equations represent holographic analogy of four wave mixing mechanism, and this mechanism inherently has the capability for correcting phase aberrations and distortion, such as those induced by turbulence in the atmosphere or in optical path. Using this mechanism, optical dynamic correlator can be built.

There two different configuration possible for performing correlation optically; the joint

transform correlator and frequency plane correlator. In our system, we adopt the frequency plane correlator which has some operational advantages.

Fig 2 shows the basic principle of frequency plane correlator using dynamic hologram. In Fig.2, u<sub>1</sub>, u<sub>2</sub> and u<sub>3</sub> represent the reference beam, reference input distribution and test input distribution, respectively. Complex modulation index m<sub>12</sub> of a phase grating produced in photorefractive material is given by

$$m_{12} = \frac{2 U_1 U_2^*}{U_1^2 + U_2^2} \quad (9)$$

where U<sub>1</sub> and U<sub>2</sub> represent the Fourier transforms of u<sub>1</sub> and u<sub>2</sub>.

The test input field U<sub>3</sub>(x,y) is diffracted by photo-induced grating to produce the output field

$$U_4 = U_2^* U_3 W \quad (10)$$

where W is a spatial frequency weighting function given by

$$W = \frac{2 A}{|U_2|^2 + I_1 + a |U_3|^2} \quad (11)$$

where a reflects the degree of interaction of the reading beam with the grating.

## 2.3. Methods of Discrimination Enhancement

In true correlation under I<sub>3</sub> >> I<sub>3</sub>, correlation output is given by

$$U_4 \approx \frac{2 U_1 U_2^* U_3}{I_1} \quad (12)$$

Therefore in case that objects of roughly the same shape or size are correlated, autocorrelation and crosscorrelation peak will be approximately same.

Correlation of two object shown in Fig.3(a) is performed by computer simulation. The programs were developed and run on a Cyber 170 computer, and FFT3D algorithm is used to calculate the complex Fourier transform of 2-D objects.

It is therefore desirable to suppress the crosscorrelation term in spatial or Fourier domain. Eq.(11) shows that by proper selection of weighting function W, the correlation U<sub>4</sub> can be enhanced remarkably.

Now we consider some methods of enhancing correlation discrimination.

### i) Edge enhancement technique

By making U<sub>2</sub> >> I<sub>1</sub>, condition which is reverse relation that of DFWM, or by high-pass filtering in spatial domain, edge enhancement can be obtained.

### ii) Grating modification method

Illuminate the modification beam into the

crystal to erase the crosscorrelation distribution.  
 iii) Thresholding method ( Fig.3 )

By using another PCM-based thresholder or amplifier , correlation peak can be thresholded or amplified.

### 3. EXPERIMENTS

To investigate the operation of pattern recognition system , the optical arrangement shown in Fig.2 was implemented. In this system , photorefractive BaTiO<sub>3</sub> single crystal of 7.56 x 5.12 x 5.48 mm, He-Ne laser of 5.5 mW and CCD line sensor or TV camera are used as a dynamic holographic matched filter , source and detector , respectively.

Experimental results are shown in Photo 1. The correlation output were obtained with a beam intensity ratio I1:I2:I3 of 0.512:1.37:0.0923. We performed experimental works of optical pattern recognition for military patterns and obtained good correlation results in real-time.

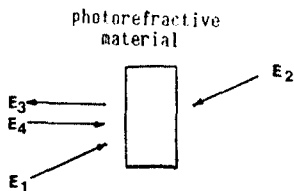


Fig.1. Basic geometry of FWM mechanism

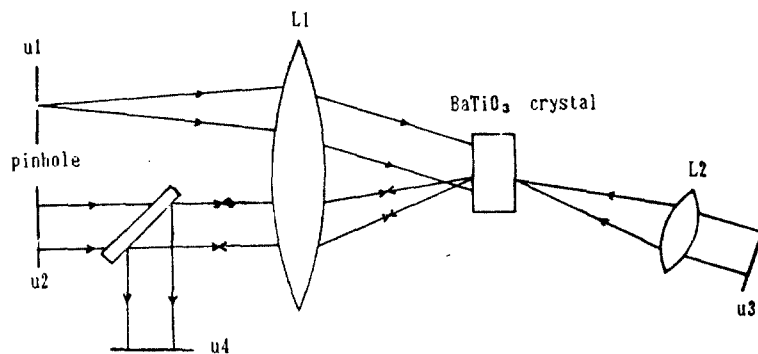


Fig.2. Frequency-plane correlator using volume holographic material

### 4. CONCLUSION

We have discussed the real-time optical pattern recognizer employing dynamic hologram in BaTiO<sub>3</sub> crystal , and some methods of enhancing correlation discrimination are also presented.

Experimental results of military patterns show that implemented system can be easily applicable to recognize high speed and high SBP images. For scale and rotation invariant operation , some technique such as anamorphic transform<sup>7</sup> should be introduced.

### REFERENCES

- [1] L.A. Vander Lugt , "Signal detection by complex spatial filtering " , IEEE Trans. on Inf. Theory , IT-10 , pp 139 ~ 145 , 1964
- [2] Ashkin , " Optically induced refractive index inhomogeneities in LiNbO<sub>3</sub> and LaTiO<sub>3</sub>" , Appl. opt. , vol.9, no.1, 72, 1966
- [3] Kukhtarev, et al, " Holographic storage in electro-optic crystal", Ferroelectric, 22, p949, 1979
- [4] J. P. Huignard and J.P. Herriau, Appl. Opt. 17, 2671, 1978
- [5] A. Yariv, et al. "Spatial convolution and correlation of optical fields via DFWM", Opt. Lett. 3, 7-9, 1978
- [6] J. Feinberg, et al, J. of Appl. phys., 51, p297, 1980
- [7] Tomasz Szoplik , " Shift-and scale-invariant anamorphic Fourier correlator", JOSA Vol.2 , No.9 , p1419 . Sept. 1985

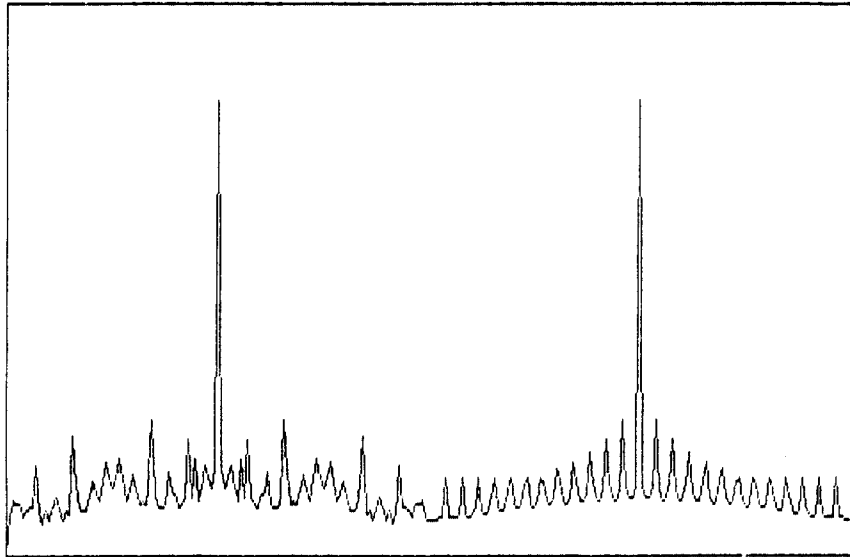
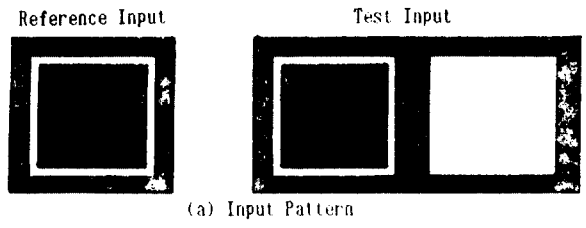


Fig.3. Correlation of similar objects

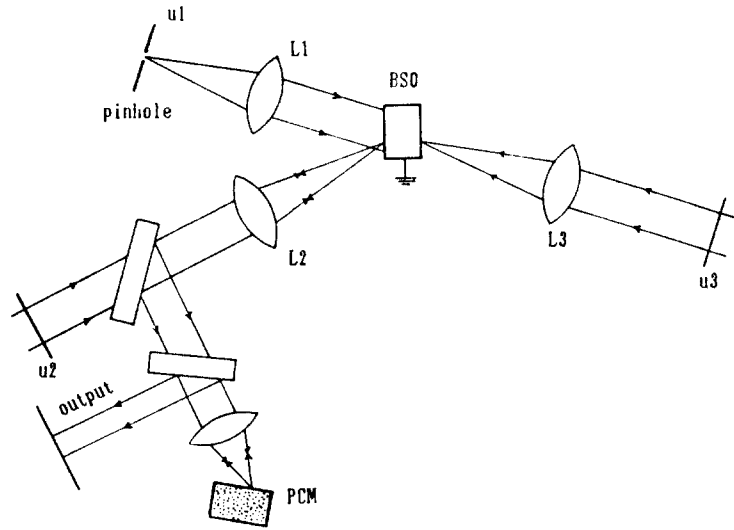
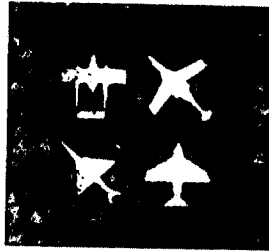
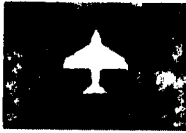


Fig.4. Thresholding Method



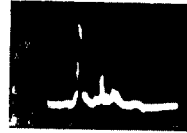
Test Input



Reference Input



TV Camera



CCD Line Sensor



Reference Input



TV Camera

(a)



Test Input



Reference Input



TV Camera

(b)

Photo 1. Experimental results